Investigation of the shape transferability of nanoscale multi-tip diamond tools in the diamond turning of nanostructures

Xichun Luo[1*], Zhen Tong[1,2], Yingchun Liang[2]

1 *Department of Design, Manufacture & Engineering Management, University of Strathclyde, Glasgow G1 1XQ, UK*

2 Center for Precision Engineering, Harbin Institute of Technology, Harbin 150001, China

**Email: Xichun.Luo@strath.ac.uk*

Abstract

In this paper, the shape transferability of using nanoscale multi-tip diamond tools in the diamond turning for scale-up manufacturing of nanostructures has been demonstrated. Atomistic multi-tip diamond tool models were built with different tool geometries in terms of the difference in the tip cross-sectional shape, tip angle, and the feature of tool tip configuration, to determine their effect on the applied forces and the machined nano-groove geometries. The quality of machined nanostructures was characterized by the thickness of the deformed layers and the dimensional accuracy achieved. Simulation results show that diamond turning using nanoscale multi-tip tools offers tremendously shape transferability in machining nanostructures. Both periodic and non-periodic nano-grooves with different cross-sectional shapes can be successfully fabricated using the multi-tip tools. A hypothesis of minimum designed ratio of tool tip distance to tip base width (L/W_f) of the nanoscale multi-tip diamond tool for the high precision machining of nanostructures was proposed based on the analytical study of the quality of the nanostructures fabricated using different types of the multi-tip tools. Nanometric cutting trials using nanoscale multi-tip diamond tools (different in L/W_f) fabricated by focused ion beam (FIB) were then conducted to verify the hypothesis. The investigations done in this work imply the potential of using the nanoscale multi-tip diamond tool for the deterministic fabrication of period and non-periodic nanostructures, which opens up the feasibility of using the process as a versatile manufacturing technique in nanotechnology.

(Some Figures in this article are in colour only in the electronic version)

Keywords: nanometric cutting; multi-tip tool; shape transferability; molecular dynamics; tool geometry; nanostructure.

1. Introduction

Recently, great interest has been shown in the fabrication of periodic micro/nano structures over large scale due to their increasing applicability in diverse research fields including optics and electronics, cell biology, bioengineering and medical science [1-3]. The advance in current nanofabrication techniques, including optical and electron beam lithography, focused ion beam (FIB) milling, nanoimprinting, and femtosecond laser machining, have boosted the development of new platforms and methodologies to produce nanostructures of targeted functions. However, these methods fail to meet the increasing interest in commercializing functional nanostructured devices due to their inherent limitations, particularly the complex processing step, low processing efficiency, and high operational costs. These limitations have created substantial interest in developing cost effective scale-up manufacturing approaches.

Diamond turning using multi-tip single crystal diamond tools, as a new machining technique, shows powerful capacity in the fabrication of micro/nano structures [4-7]. In recent decades, various kinds of micro multi-tip tools (with tool tip dimensions ranging from 15 μm to 100 μm) fabricated by the FIB milling technique were successfully applied to form well-ordered micro grooves [4-5], arrays [6], and diffraction gratings [7]. Recently nano-gratings with the pitch as lower as 150 nm were fabricated using a nanoscale multi-tip diamond tool through the diamond turning operations [8]. The effect of feed rate and the alignment issues on machining accuracy associated with the use of separate single-tip tool can be completely eliminated when using nanoscale multi-tip tools [9]. Owing to the unprecedented merits of high throughput, one-step, and highly flexible precision capabilities, this technique has led to the hope for breaking the technical bottleneck for the scale-up manufacturing nanostructures.

Nevertheless, the formation mechanism of the nanostructures as well as the relationship between the geometry of nanostructures pre-fabricated on the tool tip and the form accuracy of nanostructures replicated on the work substrate remain unclear, which has become a significant barrier to the realization of the deterministic nanomanufacturing capability. As the nanostructures are formed synchronously within a single cutting pass, the interactions of the deformed layers created by each tool tip might alter the material removal mechanism [9] and result in unpredictable processing defects. Although a few reports can be found in the literature preliminarily describing the high form accuracy and throughput of this technique [4-8], no experimental or theoretical research work has been found which investigated the dependence of

the form accuracy of machined nanostructures on the tool geometrical parameters. The characterization of the shape transferability of this technique is needed before the standardization and commercialization of nanocale multi-tip diamond tools.

Additionally, some fundamental issues related to nanometric cutting processes using the single tip diamond tool have been effectively investigated using molecular dynamics (MD) simulations method. Numerous MD nanometric cutting models were built to emulate the material removal process [10-12] and to study the effect of tool geometry on the machined surface quality [13-15]. Recently the difference in machining nanostructures between using single tip and multi-tip diamond cutting tools has also been reported [9, 16]. These studies have made a great contribution towards the in-depth understanding of the dynamic behaviour of materials under different nanometric cutting conditions. However, no pioneering research work has been developed, for nanometric cutting, to investigate the shape transferability of nanoscale multi-tip diamond tools with different tool geometries.

The present paper therefore reports systematic research on the shape transferability of nanoscale multi-tip tools with different designed tool geometries. A hypothesis of a minimum designed ratio of tip distance to tip base width (L/W_f) of the nanoscale multi-tip tool is proposed based on a theoretical study of the effect of tip distance, tip angle, and the tip configuration on the quality of machined nanostructures. Nanometric cutting experiments using nanoscale multi-tip diamond tools are then conducted to verify the hypothesis. The potential of using nanoscale multi-tip diamond tools for the deterministic scale-up fabrication of period and non-periodic nanostructures are discussed in the subsequent section.

2. MD simulation

2.1 Geometric models for MD simulations

In order to fully explore the shape transferability of nanoscale multi-tip diamond tools, four categories of diamond tool used to machine periodic and non-periodic nanostructures were studies in this paper. The cross-sectional shapes of the tools and the tip configurations are shown in Figs. 1 (a)-(d) (L is defined as the tip distance; θ is the tip angle; W_a and W_f are used to represent the width of the top and bottom of the tool tip respectively). For the purpose of concision, the four types of multi-tip tools are generally labeled as T1, T2, T3, and T4 in this paper. All of the tool models built here are based on a deformable body with

a round cutting edge radius r of $5a$ (a = 3.567 Å), a tool rake angle α of 0º, and a tool clearance angle β of 10º (as shown in Fig. 1 (e)). To save computational time, the tools were built with a double-tip to represent the multi-tip tool. The cutting processes of using 21 diamond tools with different combinations of cross-sectional geometrical parameters (listed in Table 1) are simulated in this paper.

The MD nanometric cutting model using multi-tip single crystal diamond tool is developed as shown in Fig. 1(f). The copper workpiece has dimensions of $50a_0 \times 80a_0 \times 40a_0$ (a_0 = 3.615 Å). It consists of the boundary layer and the thermostat layer with thicknesses of $2a_0$ and $3a_0$, respectively. The three orientations of the workpiece are [1 0 0], [0 1 0], and [0 0 1] in the X, Y, and Z directions respectively.

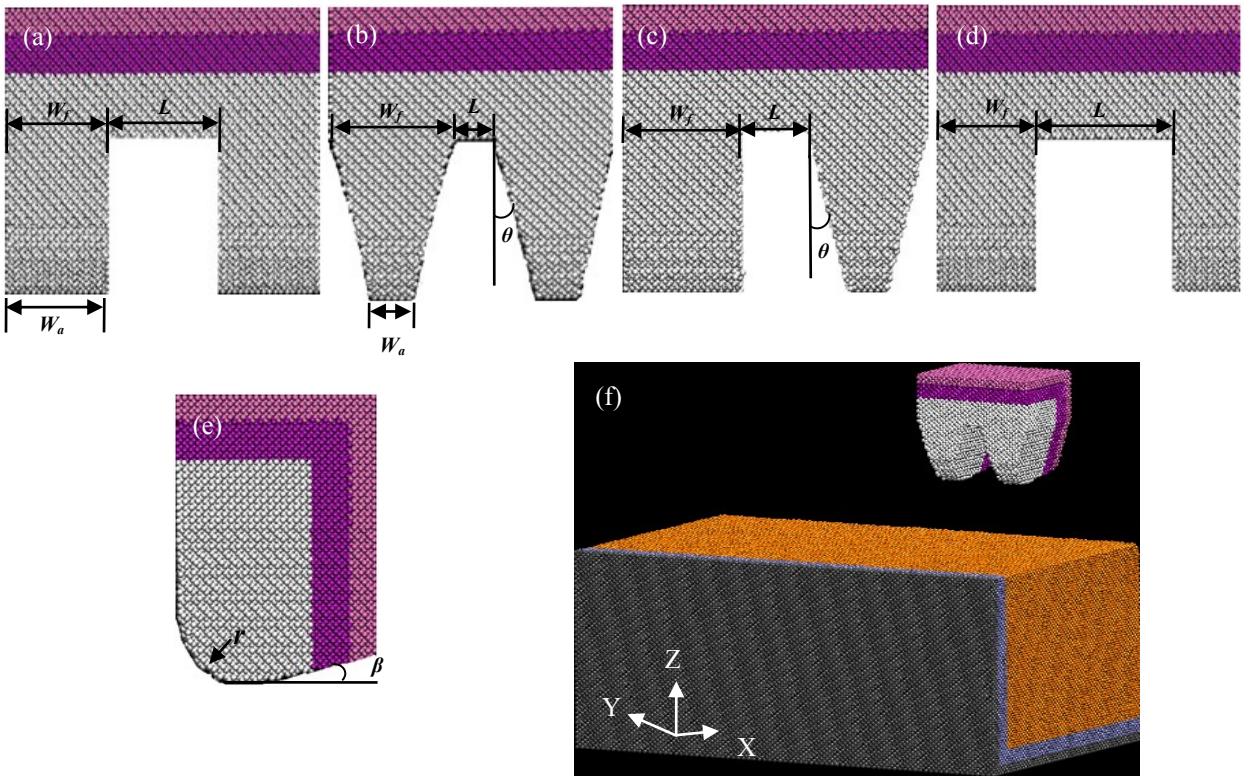

Fig. 1: Photographs of MD nanometric cutting models using multi-tip diamond tools. The front view of multi-tip tool models are (a) periodic tips configuration with rectangular cross-sectional shape (T1), (b) periodic tips configuration with trapezoidal cross-sectional shape (T2), (c) non-periodic tips configuration with a mixture of cross-sectional shapes (T3), and (d) non-periodic tips configuration with a rectangular cross-sectional shape (T4). (e) Right hand end elevation of multi-tip tool models; (f) the nanometric cutting model.

Table 1: Dimensions of nanoscale multi-tip diamond tool models (a = 3.567 Å).

	Tip distance (L)	Tip angle (θ)	Tip base width (W_f)
T1	3a, 6a, 9a, 12a, 14a	0°	9a
T2	3a, 6a, 9a, 12a, 14a	14.0°	9a
	6a	16.3°, 14.0°, 11.8°, 9.46°, 7.13°	9a
T3	3a, 5a, 7a, 9a, 12a	0°(left tip); 14.0°(right tip)	9a
T4	4a, 6a, 7a, 9a, 12a	0°	9a (left tip); 6a (right tip)

2.2 Potential functions for MD Simulation

The Embedded atom method (EAM) potential proposed by Foiles et al. [17] was used to describe the interactions between the workpeice atoms which can be expressed as:

$$E_{eam} = \sum_i F^i(\sum_{j\neq i}^{n} \rho^i(r^{ij})) + \frac{1}{2}\sum_{ij,i\neq j} \phi_{ij}(r^{ij}) \tag{1}$$

where the E_{eam} is the total energy of the atomistic system which comprises summation over the atomistic aggregate of the individual embedding energy F^i of atom i and the pair potential ϕ_{ij} between atom i and its neighboring atom j. The lower case Latin superscripts i and j refer to different atoms, r^{ij} is the distance between the atoms i and j, and $\rho^i(r^{ij})$ is the electron density of the atom i contributed by atom j.

For interactions between C-C atoms, the Tersoff potential [18] was adopted and computed as follows:

$$V_{ij} = f_C(r_{ij})[f_R(r_{ij}) + b_{ij} f_A(r_{ij})] \tag{2}$$

where V_{ij} is the bond energy of all the atomic bonds, i, j label the atoms of the system, r_{ij} is the length of the ij bond, b_{ij} is the bond order term, f_R is a two-body term and f_A includes the three-body interactions. f_C merely represents a smooth cutoff function to limit the range of the potential.

The Morse potential function [11] was used to describe the interaction between Cu-C and the total energy E_{tot} is expressed as:

$$E_{tot} = \sum_{ij} D_0 \left[e^{-2\alpha(r-r_0)} - 2e^{-\alpha(r-r_0)} \right] \tag{3}$$

where r is the instantaneous distance between atoms i and j. The cohesion energy D, the elastic modulus α, and the equilibrium bond distance r_0 are 0.087eV, 5.14 Å^{-1}, and 2.05 Å respectively.

2.3 MD simulation setup

Due to the limitation of computational power, a high cutting speed was adopted as other researchers to speed up the MD simulation. In this study all of the cutting tools were applied along the minus X direction at a constant speed of 200 m/s with a depth of cut of 2.5 nm. Two nano-grooves were formed synchronously by a single cutting pass. MD simulations were implemented by using an open source code – LAMMPS [19] compiled on a high performance computing (HPC) workstation using 32 cores. Before cutting, 85,000 computing time steps were carried out to freely relax the system to 293 K. During cutting processes, the systems were controlled by NVE ensemble and the thermostat atoms were kept at a constant temperature of 293 K through using the velocity scaling method to perform the heat dissipation [10, 11]. After the cutting, all of the models were allowed to relax for 50,000 time steps (50 ps) by holding the tool in the fixed loaded position in order to obtain the accurate form of nanostructures after elastic/plastic recovery of materials. The visualization of atomistic configurations was realized by VMD (Visual Molecular Dynamics) software. The color scheme of centro-symmetry parameter (CSP) value [9] is indicated in Table 2.

Table 2. The default value of atomic defects structure in CSP

CSP value (P)	Lattice Structure	Represent Atoms Color
3 < P < 5	Partial dislocation	Cyan
5 < P < 8	Stacking fault	Blue
8< P <21.5	Surface atoms	Orange
P> 21.5	Surface edge atoms	Pink

3. Experiment setup

In order to verify the simulation results, two nanoscale multi-tip diamond tools (different in L/W_f) were fabricated by FIB (FEI Quanta3D FEG) using the previously reported divergence compensation method [8]. The ratio of the tool tip distance to the tip base width (L/W_f) is employed as an indicator when compare the MD simulation and experimental results qualitatively. As shown in Figs. 2 (a)-(b), one is a four-tip tool with a ratio of tip distance to tip base width (L/W_f) of 1.54, and another one is a seventeen-tip tool with L/W_f of 0.33. They both have trapezoidal cross-sectional shape (tip angle θ of 14.0°) which is

the same shape as the corresponding tool tip used in the MD simulations. The nanometric cutting trials on copper substrate surfaces using the nanoscale multi-tip diamond tools were carried out on a diamond turning machine (Precitech Nanoform 250). The same cutting conditions were applied when using these two tools (cutting speed 0.03 m/s, depth of cut 100 nm). The machining process and the fabricated samples are illustrated in Figs. 2 (c) and (d). The machined surface roughness and the nanostructure pattern were measured using a white light interferometer (Form TalySurf CCI 3000) and a Scanning Electron Microscope (FEI Quanta3D FEG) respectively.

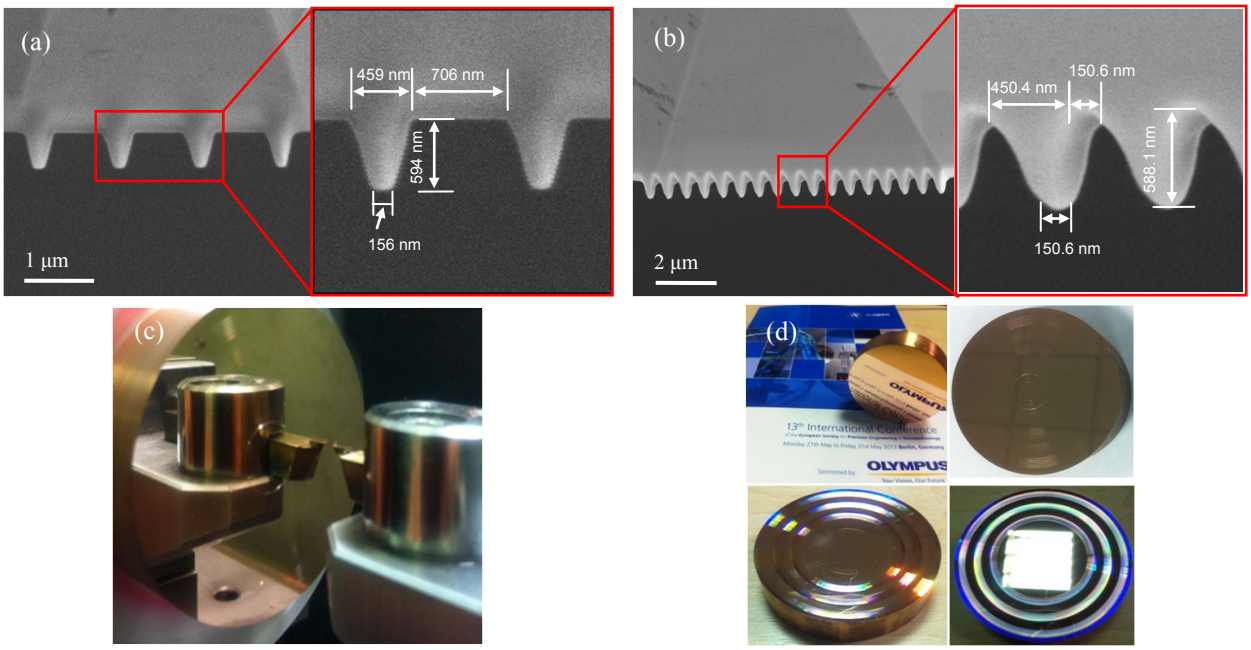

Fig. 2: Diamond turning using nanoscale multi-tip diamond tools: (a) SEM image of multi-tip tool with L/W_f of 1.54; (b) SEM image of multi-tip tool with L/W_f of 0.33; (c) nanometric cutting operation; (d) the machined surfaces with nanostructures.

4. Results and discussion

4.1 Formation of periodic and nonperiodic nanostructures

Fig. 3 shows the nano-grooves fabricated by using the four types of nanoscale multi-tip diamond tools with the designed tip distance L being $12a$ ($L/W_f = 1.33$). The atoms with cyan and blue color represent the particle dislocations and stacking faults, respectively. As is evident from Fig. 3 (the left and middle columns), nano-grooves with different cross-sectional shapes were formed synchronously within a single cutting pass through material plastic deformation dominated by the dislocation nucleation and the

extension of the stacking faults [9]. The quality of the machined nanostructures was characterized by both the form accuracy of the machined nanostructures and the thickness of the deformed layers. It is found that the thicknesses of the deformed layer are 4.8 nm and 4.5 nm for type T1 and T2 tools, respectively. However, slightly larger values of 5.0 nm and 5.3 nm were found when type T3 and T4 tools were applied. The results suggest that tools of periodic tip configuration might have better shaping performance than tools with non-periodic tip configuration.

Moreover, the pictures located at the right column of Fig. 3 show the cross-sectional views of the machined nano-grooves after a full relaxation process. The form error was evaluated by the divergence from the machined nano-grooves to the designed shapes. It is found that the form errors of using different types of multi-tip tools are all less than 7.3%, which demonstrates the high machining capacity of using this technique for the fabrication of periodic and non-periodic nanostructures. Further, apparently material elastic recovery was observed when the trapezoidal tips were used (Figs. 3 (b) and (c)). These results suggest that employing a tool tip angle would create a heterogeneous distribution of the compressive residual stress at the side walls of the machined nano-grooves. The effect of tool tip angle on the integrity of the machined nanostructures will be further discussed in the following section.

Additionally, the averaged cutting forces at a steady cutting state are summarized in Fig. 4. The cutting forces were obtained by summing the forces of tool atoms and the directions of cutting forces are illustrated in Fig. 4 (a). It was found that both the tangential cutting force F_x and normal cutting force F_z of using rectangular cross-sectional shape tools (T1 and T4) were larger than when using trapezoidal cross-sectional shape tool (T2). The value of F_x when using the multi-tip tool with the mixture of tool tip shapes (T3) was 68.2 nN, which was slightly larger than the mean value of the tangential cutting forces (being 65.6 nN) when the T1 and T2 type tools were used . Moreover, the ratios of F_z / F_x were around 0.7 when the T1 and T4 type tools were used. However, the ratios of F_z / F_x increased to 1.0 when T2 and T3 type tools were used. The results indicate that trapezoidal tips can minimize the tangential cutting forces and thus increase the ratio of F_z / F_x. The apparently smaller cutting forces when using the T2 type tool suggest that the periodic trapezoidal cross-sectional shape multi-tip tool offers the best shape transferability among the tools studied in the present paper.

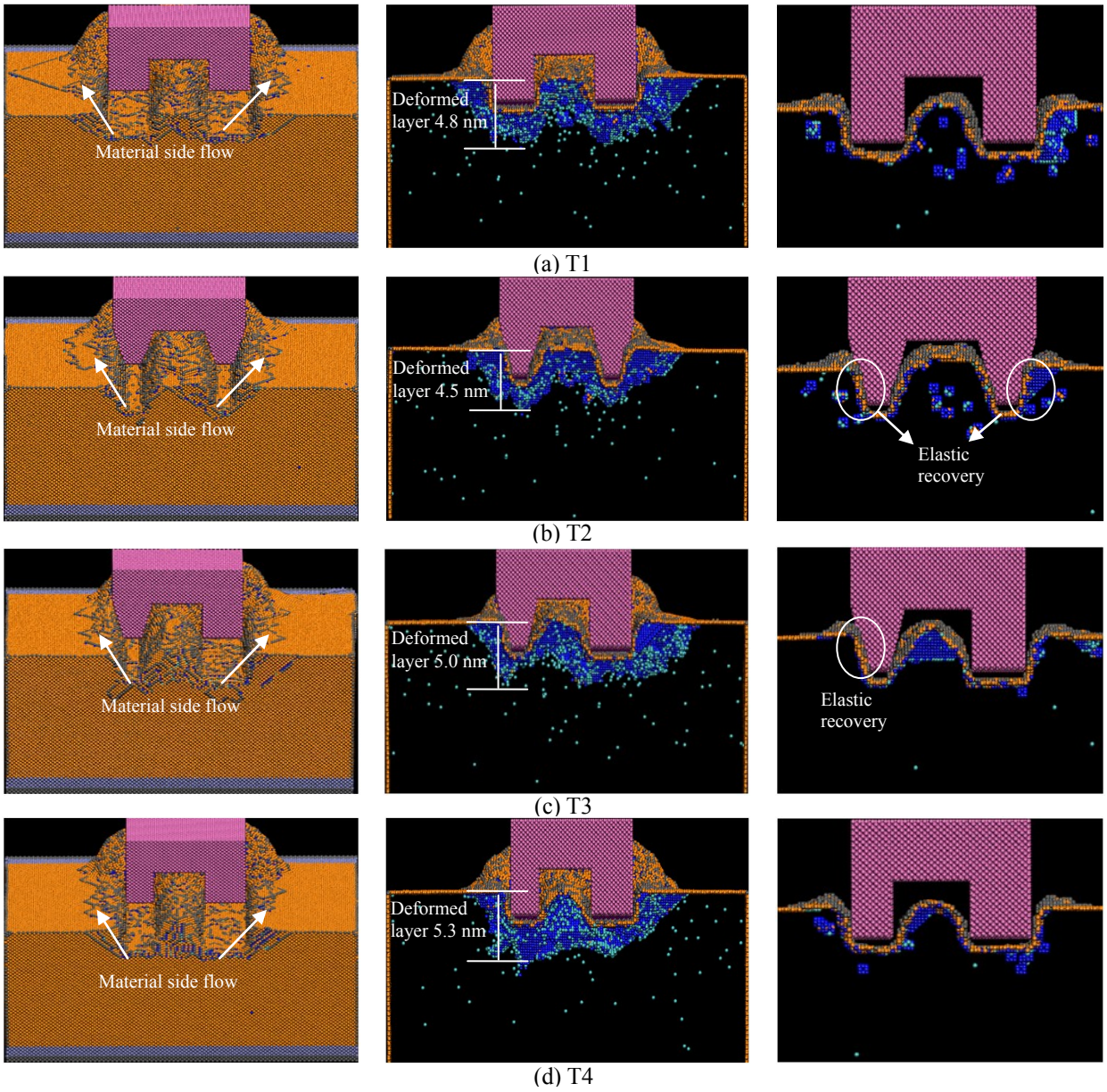

Fig. 3: Photographs of the nanostructures generated (left), the cross-sectional views of the deformed layer (middle), and the cross-sectional views of the shape of the machined nano-grooves (right) when using four types of nanoscale multi-tip diamond tools, labeled as: (a) T1, (b) T2, (c) T3, and (d) T4. (Tip distance L 12a, depth of cut 2.5 nm, cutting speed 200 m/s. Cyan and blue atoms represent particle dislocation and stacking fault, respectively.)

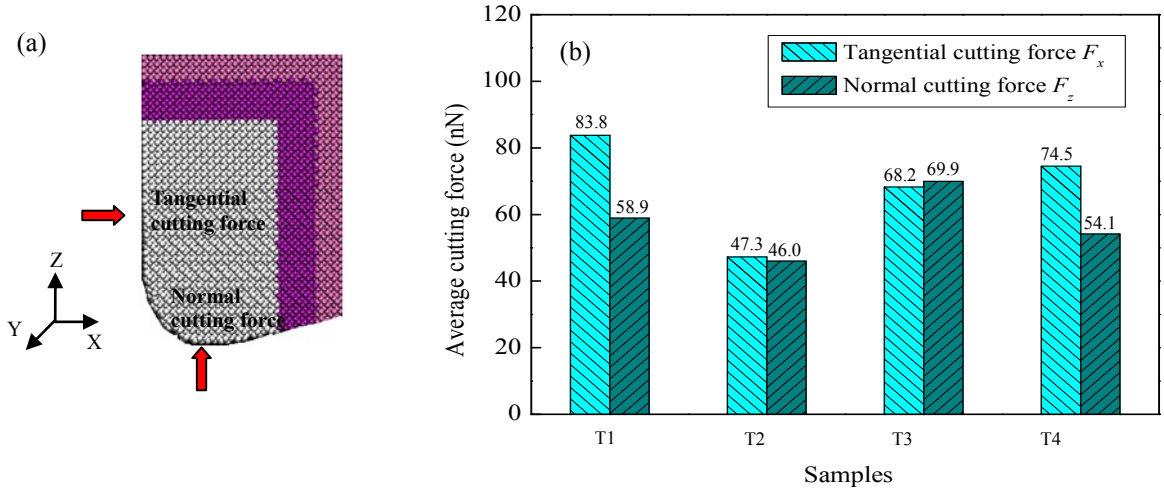

Fig. 4: Cutting force during the nanometric cutting process: (a) direction of cutting forces; (b) averaged cutting forces generated when using different types of cutting tools.

4.2 Denpendence of the shape transferability on the tool geometry

The cross-sectional shape of the tool tip and the tip distance are two major geometrical parameters when designing the nanoscale multi-tip cutting tool. In order to quantify the effect of tool geometry on the shape transferability, a series of MD nanometric cutting simulations were carried out while varying the tip distance of diamond tools (as summarized in Table 1).

Fig 5 shows the photographs of cross-sectional views of nano-grooves generated by multi-tip diamond tools of different tool tip distances (type T1 tools). It is found that the quality of the machined nano-grooves improves with the increase of the ratio of L/W_f. As shown in Figs. 5(a) and (d), a large form error was found when L is $6a$ ($L/W_f = 0.67$). Similar results were observed when L equals $3a$ (not shown in this paper for the purpose of concision). However, the nano-grooves can be well formed when the tip distance is equal to or greater than $9a$ ($L/W_f \geqslant 1$). Moreover, as shown in Figs. 5(e)-(f), the thickness of the deformed layer was found to be decreased with the increase of tool tip distance. The results preliminarily suggest that, for the nanoscale multi-tip tool cutting, there exists a limit of the ratio of L/W_f which can be used to achieve high form accuracy in a single cutting pass.

The cross-sectional views of nano-grooves generated by tools with different tip angles (tool type T2) are shown in Fig. 6. In order to quantify the effect of the tip angle, the tools were built with the same ratio of L/W_f (0.67). Similarly to the rectangular cross-sectional shape tool cutting, large form errors were found

when a tip angle of 7.13° was used. However, as is evident from Figs. 6(e) and (f), the nano-grooves can be accurately formed when the tip angle is equal to or greater than 11.8°. The deformed layers were found to be decreased with the increase of the tip angle. Thus, applying a multi-tip diamond tool with the proper tool tip angles, the shape transferability can be improved significantly.

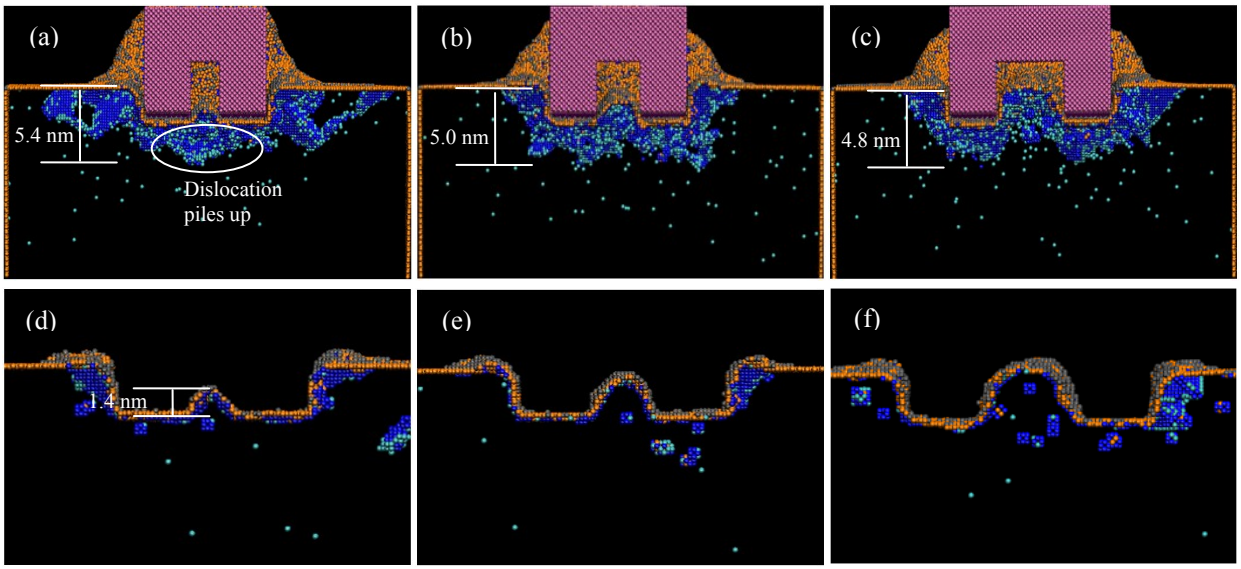

Fig. 5: Photographs of cross-sectional views of deformed layers when using multi-tip tools with different tip distances: (a) L6 nm, (b) L9 nm, and (c) L12 nm; and the corresponding views of machined nano-grooves ((d)-(f)). Cyan and blue atoms represent particle dislocation and stacking fault, respectively.

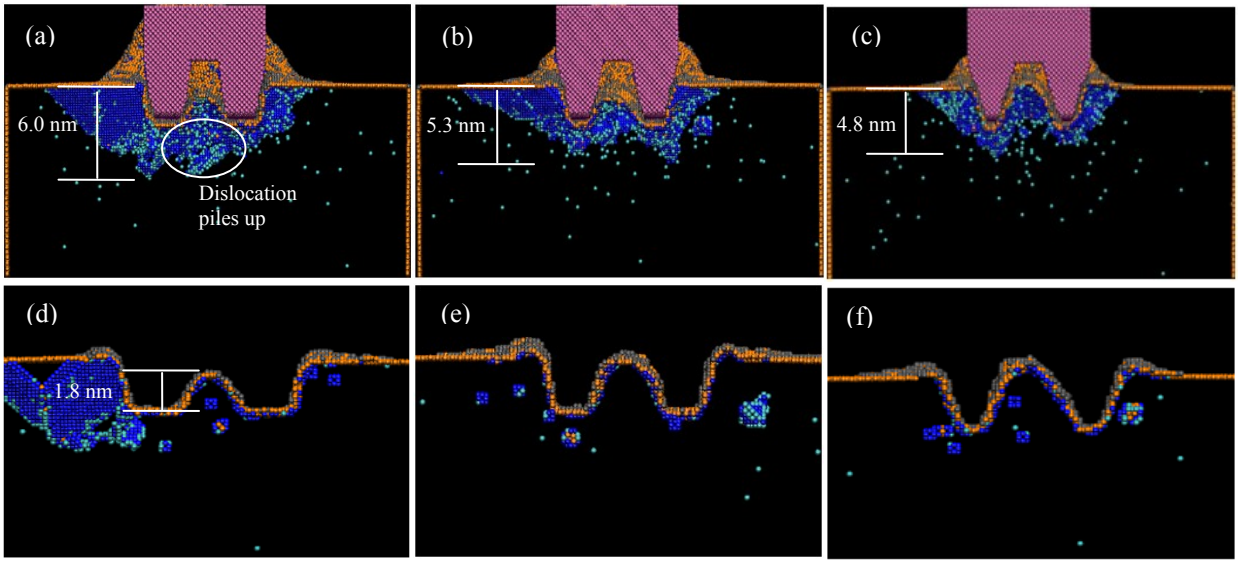

Fig. 6: Photographs of deformed layer during nanometric cutting process when using multi-tip tools with different tip angles: (a) 7.13°, (b) 11.8°, and (c) 16.3°; and the corresponding views of machined nano-grooves ((d)-(f)). The ratios of L/W_f of the tools are 0.67. Cyan and blue atoms represent particle dislocation and stacking fault, respectively.

Moreover, the variation of the form errors of the machined nano-grooves with the ratio of L/W_f of the four

types of multi-tip tools is summarized in Fig. 7. It was found that the form errors all decreased with the ratio of L/W_f. A critical form error of 10 % can be defined as the upper limit of the deviation of the machined nano-grooves (as indicated by the dashed line in Fig. 7), and the corresponding critical ratios of L/W_f are 0.93, 0.53, 0.76, and 0.97 for T1, T2, T3 and T4 type tools respectively. The results indicate that the multi-tip tools with trapezoidal tips (T2) have better shape transferability than rectangular cross-sectional shape tools (T1 and T4); and multi-tip tools with periodic tip configuration (T1 and T2) have better shape transferability than those with non-periodic tip configuration (T3 and T4). The shape transferability for tools with mixed shape tips (T3) depends significantly on the geometry of the two adjacent tool tips. The critical ratio of L/W_f lies between the L/W_f ratio of the two adjacent tips calculated from the periodic tip configurations (T1 and T2).

The reasons accounting for the difference are as follows. Since the nano-grooves are formed synchronously in the nanoscale multi-tip tool cutting, the overlap of the deformed layers created by cutting tips should be well controlled [9]. When the tool cuts into the workpiece, each tip will create a deformed layer in its immediate vicinity (also named as work-affected layer). The range of the plastically deformed region is two to ten times the indention radius [20]. Because the trapezoidal cross-sectional shape tip has a smaller contact radius in the YOZ plane as compared to the rectangular cross-sectional shape tip, a smaller region of work-affected area is formed [20-21]. Thus the overlap of the deformed layer can be effectively minimized when using tools with trapezoidal cross-sectional shape tips. Moreover, the material side flow made a significant contribution to the formation of the nanostructures [9, 21]. As the tool with periodic tip configuration has better central symmetry properties than the tool with non-periodic tips configuration, a uniform material side flow is easily achieved and therefore a smaller critical ratio of L/W_f is required. Additionally, under the same cutting conditions, smaller cutting forces were observed when using trapezoidal cross-sectional shape tips with periodic tips configuration (as discussed in section 4.1). Thus, it is concluded that the tool geometry of nanoscale multi-tip diamond tools has a significant influence on the quality of machined nanostructures. The tool tip angle can effectively control the material side flow [15, 21] and minimize the interactions of deformed layers beneath the tool tips during the machining process. A minimum ratio of L/W_f should be met for the high precision machining of nanostructures based on the MD simulation results discussed above. The next

section will further verify this hypothesis through nanomectic cutting trials using nanoscale multi-tip diamond tools.

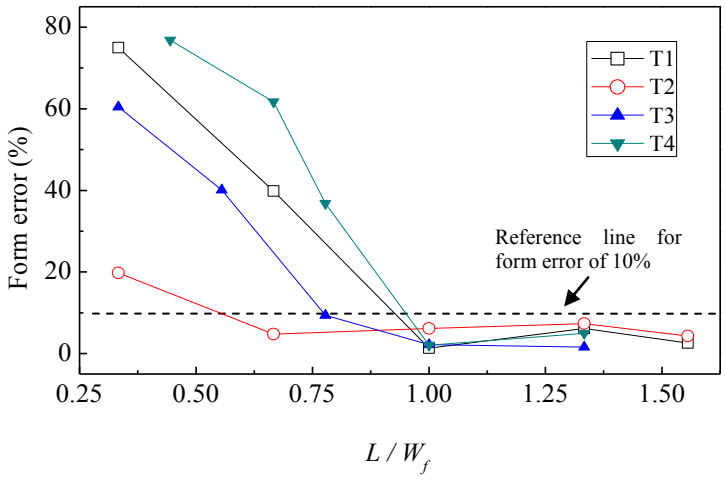

Fig. 7: The variation of the form error of machined nano-grooves with the ratio of L/W_f of the four types of multi-tip diamond tools.

4.3 Experimental verification

Since the MD simulation results show that the periodic trapezoidal cross-sectional shape offers the best shape transferability, two nanoscale multi-tip diamond tools with such configuration were used in the cutting trials. The L/W_f ratios of these two diamond tools are 1.54 and 0.33. Two sets of experiments were carried out to evaluate the hypothesis proposed based on the MD simulations. In the first experiment, a series of four parallel nano-grooves were successfully formed by the multi-tip tool with L/W_f ratio of 1.54 (as shown in Fig8 (a)). The form accuracy of the machined nano-grooves is preliminarily characterized as the deviation of the measured width of nano-grooves (averaged width is 203 nm) to the width of the multi-tip tool (the tip width is 207 nm at the tip height of 100 nm). The divergence value of 4 nm is mainly due to the elastic recovery of the work material after the tool tip is released from the machined surface [8-9]. The small form error demonstrates the high machining capacity of using the nanoscale multi-tip tool to cut well-defined trapezoidal nano-grooves on a copper surface. The same cutting operation was then applied for the second multi-tip tool cutting ($L/W_f = 0.33$). As is evident from Fig. 8 (b), nano-grooves were fabricated with serious processing defects in terms of side burrs and structural damages. Thus, the experimental results qualitatively confirm the hypothesis predicated by MD simulations.

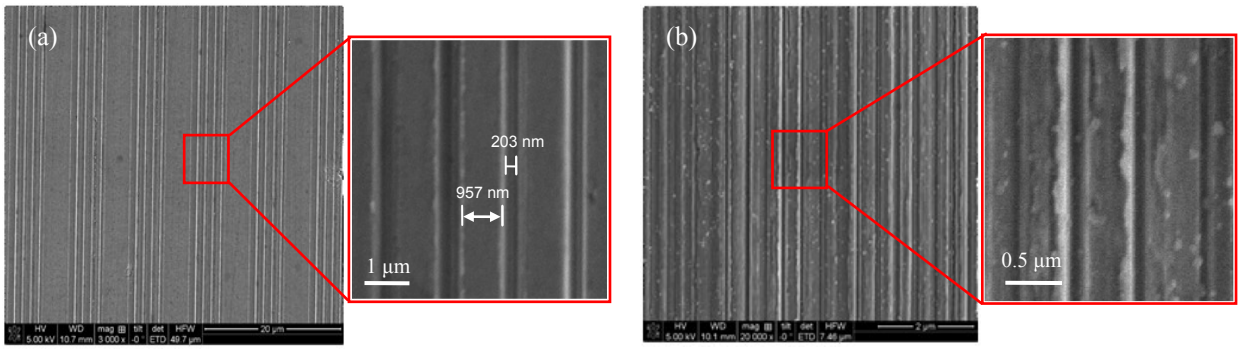

Fig. 8: SEM images of the nanostructures fabricated by nanoscale multi-tip diamond tools with different ratio of tip distance to tip base width (L/W_f): (a) L/W_f 1.54; (b) L/W_f 0.33. (Cutting speed 0.03 m/s, depth of cut 100 nm, feed rate 9 μm/rev).

Nevertheless, it is noted that the critical value of the ratio of tool tip distance to tool tip width (L/W_f) need be clarified through more quantitative experiment and theoretical analysis in the future. Currently, it is still quite difficult to compare MD simulation and experimental results in the same spatial and time scale. The difficulties in answering this fundamental question from experimental side have been the limitation of using FIB to fabricate multi-tip diamond tool in several nanometers, and the time resolution that is needed for a detection equipment to capture the transient process of defects formation which evolve on time scales of some nanoseconds. On the MD simulation side the difficulties lie in developing a super high performance computing system for solving a highly inhomogeneous many body problem in the same spatial and time scales as experiments, as well as an effective visualization technique for analyzing the MD simulation results.

In order to overcome these limitations, in present study the ratio of tool tip distance to tool tip width (L/W_f) was employed as an indicator when qualitatively compare the results between the MD simulation and the experiments focusing on the dimensional accuracy of machined nanostructures. As the plastic deformation zone below the cutting tool tip also increases with the increase of the size of the tool tip, this assumption is reasonable at current spatial scale.

Moreover, Komanduri et al. [22] commented that the effect of high cutting speed used in MD simulations can be minimized when analysis the general nature of the process. In present work, the phenomenon of formation of nanostructures observed from the MD simulation is in good agreement with the initial experimental test. This result shows the effect of adopting high cutting speed in MD simulation can be ignored.

Theoretically, based on Hill's elastic—plastic theory Taniguchi [20] has proposed a method of using c/a, the ratio between the radii of the plastically deformed zone and the indentation, to determine the extent of plastically deformed zones as schematically shown in Fig. 9. The value of c/a is calculated as follows:

$$\left(\frac{c}{a}\right)^3 = \frac{E}{3(1-\upsilon)Y} \tag{4}$$

where E is the modulus of elasticity, Y is the yield stress, and υ is the Poisson's ratio. For a ductile metal material such as copper, the measured c/a ratio is around 8.0 [20] which theoretically predicts that the deformed layer during the nanometric cutting of copper would have a thickness of up to eight times the contact radius of the tool tip. For single tip tool cutting, it is reported that the deformed layer of the lateral cutting pass will reshape the former machined nanostructures if the distance between the two cutting passes is smaller than a critical value [9, 11-12]. For multi-tip tool cutting, this feed rate issue can be avoided because the nanostructures are formed synchronously by multiple tips with a single cutting pass [9]. However, this advantage only works when the ratio L/W_f of the multi-tip tool is larger than a critical value. Below this value, the overlap of the deformed layers created by each tool tip might affect the material plastic flow and degrade the form accuracy of the machined nanostructures. Because a tool with trapezoidal cross-sectional shape tips would create a smaller region of the deformed layer than a tool with rectangular tips, a smaller tip distance can be used in the tool design process. In addition, the overlap of the deformed layers has been vividly evidenced by the MD simulation results showing the dislocation pile-ups beneath the tool tips (as shown in Figs. 5 and 6).

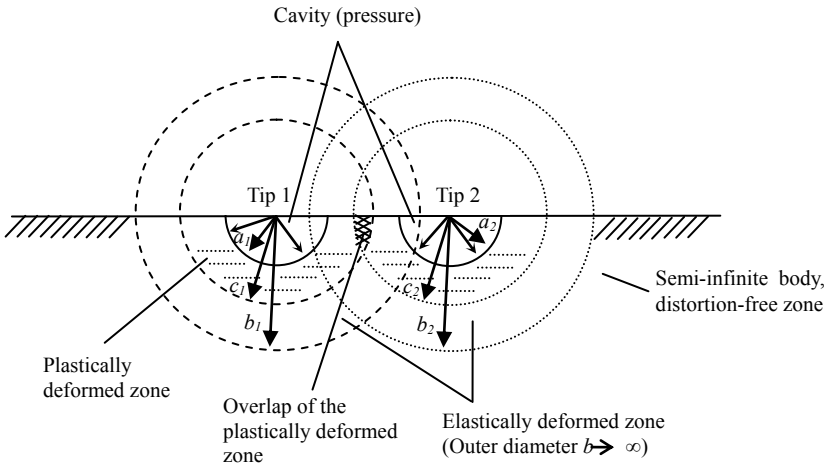

Fig. 9: Schematic illustration of the overlap of the deformed zone during a multi-tip tool cutting process based on Hill's shell expansion theory.

In general, any complex tool face geometry is possible. As the tools and the machined structures are in a range of sub-microns or dozens of nanometers, minimum processing defects caused by the improper design of the tool geometry might seriously degrade the form accuracy of machined nanostructures. Nevertheless, as evidenced by both the experimental results and the simulation data presented here, when the value of L/W_f of the tool is sufficiently large, the side effect of the overlap of deformed layers can be minimized or even totally overcome. This result indicates the great potential of improving the form accuracy of nanostructures by minimizing the overlap of work-affected layers through an optimal design of the geometry of nanoscale multi-tip diamond tools — a feature that needs to be further explored and developed in future work.

5. Conclusions

In this work, the shape transferability of using nanoscale multi-tip diamond tools has been studied. The conclusions are drawn as follows:

(1) The simulation results demonstrate the high processing capacity of nanoscale multi-tip diamond tools in term of the dimensional accuracy of machined nanostructures. High precision periodic and non-periodic nano-grooves with various kinds of cross-sectional shapes can be well formed within a single cutting pass.

(2) The tool tip angle of the nanoscale multi-tip diamond tool has a significant influence on the quality of machined nanostructures. In present work, a multi-tip tool with a tip angle equal to or greater than 11.8°

can improve the form accuracy of nanostructures by reducing the cutting force and the interactions of deformed layers beneath the tool tips.

(3) The periodic tip configuration has better shape transferability than the non-periodic tip configuration. The ratio of tool tip distance to tip base width should be carefully considered when designing nanoscale multi-tip diamond tools.

(4) The overlap of the work-affected layers significantly affects the shaping capacity of nanoscale multi-tip tools. An optimal design of tool tip angle and tool tip distance provides a potential measure to improve the form accuracy of machined nanostructures in future work.

Acknowledgment

The authors gratefully acknowledge the financial support from EPSRC (EP/K018345/1) and the National Funds for Distinguished Young Scholars (No.50925521) of China. The authors would also like to acknowledge the Centre for Precision Technologies at the University of Huddersfield for the access to Precitech Nanoform 250 UltraGrind machine in this study, and Prof. Frank Travis for the proof reading of this manuscript.

References

[1] P. Bartolo, J.P. Kruth, J. Silva, G. Levy, A. Malshe, K. Rajurkar, M. Mitsuishi, J. Ciurana, M. Leu, Biomedical production of implants by additive electro-chemical and physical processes *CIRP Annals - Manufacturing Technology* 2012 **61**(2) 635–655

[2] D. Berman, J. Krim, Surface science, MEMS and NEMS: Progress and opportunities for surface science research performed on, or by, microdevices *Prog. Surf. Sci.* 2013 **88** 171–211

[3] I.P. Kaur, H. Singh, Nanostructured drug delivery for better management of tuberculosis *J. Control. Release* 2014 **184** 36–50

[4] Y.N. Picard, D.P. Adams, M.J. Vasile, M.B. Ritchey, Focused ion beam-shaped microtools for ultra-precision machining of cylindrical components *Precis. Eng.* 2003 **27** (1) 59–69

[5] S.J. Kim, D. Le, S.W. Lee, K.H. Song, and D.Y. Lee, Experiment-based statistical prediction on diamond tool wear in micro grooving Ni-P alloys *Diamond & Relat. Mater.* 2014 **41** 6–13

[6] X Ding, G C Lim, C K Cheng, David Lee Butler, K C Shaw, K Liu and W S Fong, Fabrication of a micro-size diamond tool using a focused ion beam *J. Micromech. Microeng.* 2008 **18** 075017

[7] Z.W. Xu, F.Z. Fang, S. J. Zhang, X. D. Zhang, X. T. Hu, Y. Q. Fu, L. Li, Fabrication of micro DOE using micro tools shaped with focused ion beam *Opt. Expr.* 2010 **18** (8) 8025–8032

[8] J Sun, X Luo, W Chang, M J Ritchie, J Chien and A Lee, Fabrication of periodic nanostructures by single-point diamond turning with focused ion beam built tool tips *J. Micromech. Microeng.* 2012 **22** 115014

[9] Zhen Tong, Yingchun Liang, Xiangqian Jiang, Xichun Luo, An atomistic investigation on the mechanism of machining nanostructures when using single tip and multi-tip diamond tools *Appl. Surf. Sci.* 2014 **290** 458–465

[10] Q.X. Pei, C. Lu, H.P. Lee, Y.W. Zhang, Study of Materials Deformation in Nanometric Cutting by Large-scale Molecular Dynamics Simulations *Nanoscale Res. Lett.* 2009 **4** 444–451

[11] Yongda Yan, Tao Sun, Shen Dong, Yingchun Liang, Study on effects of the feed on AFM-based nano-scratching process using MD simulation *Comput. Mater. Sci.* 2007 **40** (1) 1–5

[12] T.H. Fang, C.I. Weng, J.G. Chang, Three-dimensional molecular dynamics analysis of processing using a pin tool on the atomic scale *Surf. Sci.* 2000 **501** 138–147

[13] P. Z. Zhu, Y. Z. Hu, T. B. Ma, and H. Wang, Study of AFM-based nanometric cutting process using molecular dynamics *Appl. Surf. Sci.* 2010 **256** (23) 7160–7165

[14] QX Pei, C Lu, FZ Fang, H Wu, Nanometric cutting of copper: A molecular dynamics study *Comput. Mater. Sci.* 2006 **37** (4) 434–441

[15] Tauhiduzzaman M, Veldhuis SC, Effect of material microstructure and tool geometry on surface generation in single point diamond turning *Precis Eng*, 2014 **38** (3) 481–491

[16] Zhen Tong, Yingchun Liang, Xuechun Yang, Xichun Luo, Investigation on the thermal effects during nanometric cutting process while using nanoscale diamond tools Int. J. Adv. Manuf. Technol., 2014, **74** 1709–1718

[17] S. M. Foiles, M. I. Baskes and M. S. Daw, Embedded-atom-method functions fo the fcc metals Cu, Ag, Au, Ni, Pd, Pt, and their alloys *Phys. Rev. B.* 1986 **33** 7983–7991

[18] J. Tersoff, Modeling solid-state chemistry: Interatomic potentials for mnlticomponent systems *Phys Rev B,* 1989 **39**(8) 5566–5568

[19] S.J. Plimpton, Fast parallel algorithms for short range molecular dynamics *J. Comp. Phys.* 1995 **117** 1–19

[20] Hiromu N., *Principles of Precision Engineering*, Translated by Ryu T. (New York: Oxford University Press) 1994 pp 251–252

[21] Kai Liu, Shreyes N. Melkote, Effect of plastic side flow on surface roughness in micro-turning process *Int.J. Machine Tools & Manufacture,* 2006 **46** 1778–1785

[22] R. Komanduri, N. Chandrasekaran, L. M. Raff, Molecular dynamics simulation of the nanometric cutting of silicon, *Philosophical Magazine B,* 2001 **81** 1989-2019.